Experimental and Theoretical Study of Reaction of OH with 1,3-Butadiene

Zhuangjie Li,*,† Phu Nguyen,† Maria Fatima de Leon,† Jia Hia Wang,‡ Keli Han,‡ and Guo Zhong He‡

Department of Chemistry and Biochemistry, California State University-Fullerton, Fullerton, California 92834, and State Key Laboratory of Molecular Reaction Dynamics, Dalian Institute of Chemical Physics, Chinese Academy of Sciences, Dalian 116023, China

Received: October 4, 2005; In Final Form: November 29, 2005

The kinetics of the reaction of hydroxyl radical with 1,3-butadiene at 240−340 K and a total pressure of ∼1 Torr has been studied using relative rate combined with the discharge flow and mass spectrometer technique. The reaction dynamics of the same reaction has also been investigated using ab initio molecular orbital theory. The rate constant for this reaction was found to be negatively dependent on temperature, with an Arrhenius expression of $k_1 = (1.58 \pm 0.07) \times 10^{-11} \exp[(436 \pm 13)/T]$ cm^3 molecule^{-1} s^{-1} (uncertainties taken as 2σ), which was in good agreement with that reported by Atkinson et al.[21] and Liu et al.[22] at 299−424 K. Mass spectral evidences were found for the addition of OH to both the terminal and the internal carbons of 1,3-butadiene. Our computational results suggest that both addition of OH to 1,3-butadiene and the abstraction of hydrogen atom from 1,3-butadiene by the OH radical are exothermic processes and that the addition of OH to the terminal carbon of the 1,3-butadiene is predicted to have an activation energy of 0.7 kcal mol^{-1}, being the most energetically favored reaction pathway.

1. Introduction

1,3-Butadiene is currently ranked 36th in the top 50 most produced chemicals in the United States. It has been widely used in the chemical industry as a major component of man-made rubber, resins, and plastics.[1] This compound has been emitted into the atmosphere from a number of sources including tobacco smoke, automobile exhaust, and gasoline,[2−4] and concentration of 1,3-butadiene at parts per billion levels has been found in ambient urban air.[5−9] 1,3-Butadiene is considered as a significant toxic pollutant. It has been included in the list of 189 chemicals that are specified as hazardous air pollutants under the 1990 U.S. Clean Air Act Amendments. It is also on California's list of toxic air contaminants.[1,10] Its carcinogenic and mutagenic properties in humans have been recognized, and photochemical conversion of 1,3-butadiene to genotoxic products in the presence of nitrogen oxides has also been acknowledged.[11−14] A quantitative assessment for lifetime cancer risk made by the U.S. EPA has shown that the unit risk factor for 1,3-butadiene is more than 30 times that of benzene.[15]

It is necessary to understand the atmospheric transformations of 1,3-butadiene in order to integrate its transformations into air quality models for toxic species and to improve regulatory quantitative risk decision-making analysis. 1,3-Butadiene is removed from the atmosphere mainly by reacting with radical species such as OH, NO_3, and Cl atoms.[9,16] The reaction of 1,3-butadiene with O_3 may also be a tropospheric sink for this molecule.[9,16] It is expected that the hydroxyl radical is a primary reactive species responsible for the daytime removal of 1,3-butadiene from the atmosphere because of its high reactivity toward a variety of volatile organic compounds (VOCs) including alkenes[17−23]

$$CH_2{=}CH{-}CH{=}CH_2 + OH \rightarrow \text{products} \quad (1)$$

Atkinson et al.[21] measured the absolute rate constant for reaction 1 at 100 Torr in Ar over a temperature range of 299−424 K using a flash photolysis-resonance fluorescence technique. They reported a rate constant of $(6.85 \pm 0.69) \times 10^{-11}$ cm^3 molecule^{-1} s^{-1} for reaction 1 at room temperature and an Arrhenius expression of $k_1 = 1.45 \times 10^{-11} \exp[(930 \pm 300)/RT]$ cm^3 molecule^{-1} s^{-1}. Liu et al.[22] also measured the absolute rate constant for reaction 1 at 1 atm in Ar at 305−1173 K using resonance fluorescence technique. They reported an Arrhenius expression to be $k_1 = (1.4 \pm 0.1) \times 10^{-11} \exp[(440 \pm 40)/T]$ cm^3 molecule^{-1} s^{-1} at temperatures below 600 K. Above 600 K, the rate constant for the reaction 1 was reported to decrease markedly with increasing temperature.[22] To our knowledge there is no kinetic data available for the reaction 1 at tropospheric temperatures of $T < 298$ K, and the atmospheric lifetime of this compound was previously suggested to be a few hours based on the available kinetic data at $T \geq 298$ K.[23] Since most OH radical involved reactions take place in the atmosphere at temperatures lower than 298 K, it is necessary to acquire kinetic information on reaction 1 at temperatures representative of troposphere to accurately model atmospheric chemistry. Mechanistically the reaction of OH with 1,3-butadiene has several possible reaction pathways

$$CH_2{=}CH{-}CH{=}CH_2 + OH \rightarrow C(OH)H_2{-}\bullet CH{-}CH{=}CH_2 \leftrightarrow C(OH)H_2{-}CH{=}CH{-}\bullet CH_2 \ (\mathbf{P1}) \quad (1.1)$$

$$\rightarrow \bullet CH_2\text{-}C(OH)H{-}CH{=}CH_2 \ (\mathbf{P2}) \quad (1.2)$$

$$\rightarrow CH\bullet{=}CH{-}CH{=}CH_2 + H_2O \ (\mathbf{P3}) \quad (1.3)$$

$$\rightarrow CH_2{=}C\bullet{-}CH{=}CH_2 + H_2O \ (\mathbf{P4}) \quad (1.4)$$

* To whom correspondence should be addressed. Phone: 714-278-3585. Fax: 714-626-8010. E-mail: zli@fullerton.edu.
† California State University, Fullerton.
‡ Chinese Academy of Sciences.

10.1021/jp0556557 CCC: $33.50
Published on Web 02/08/2006

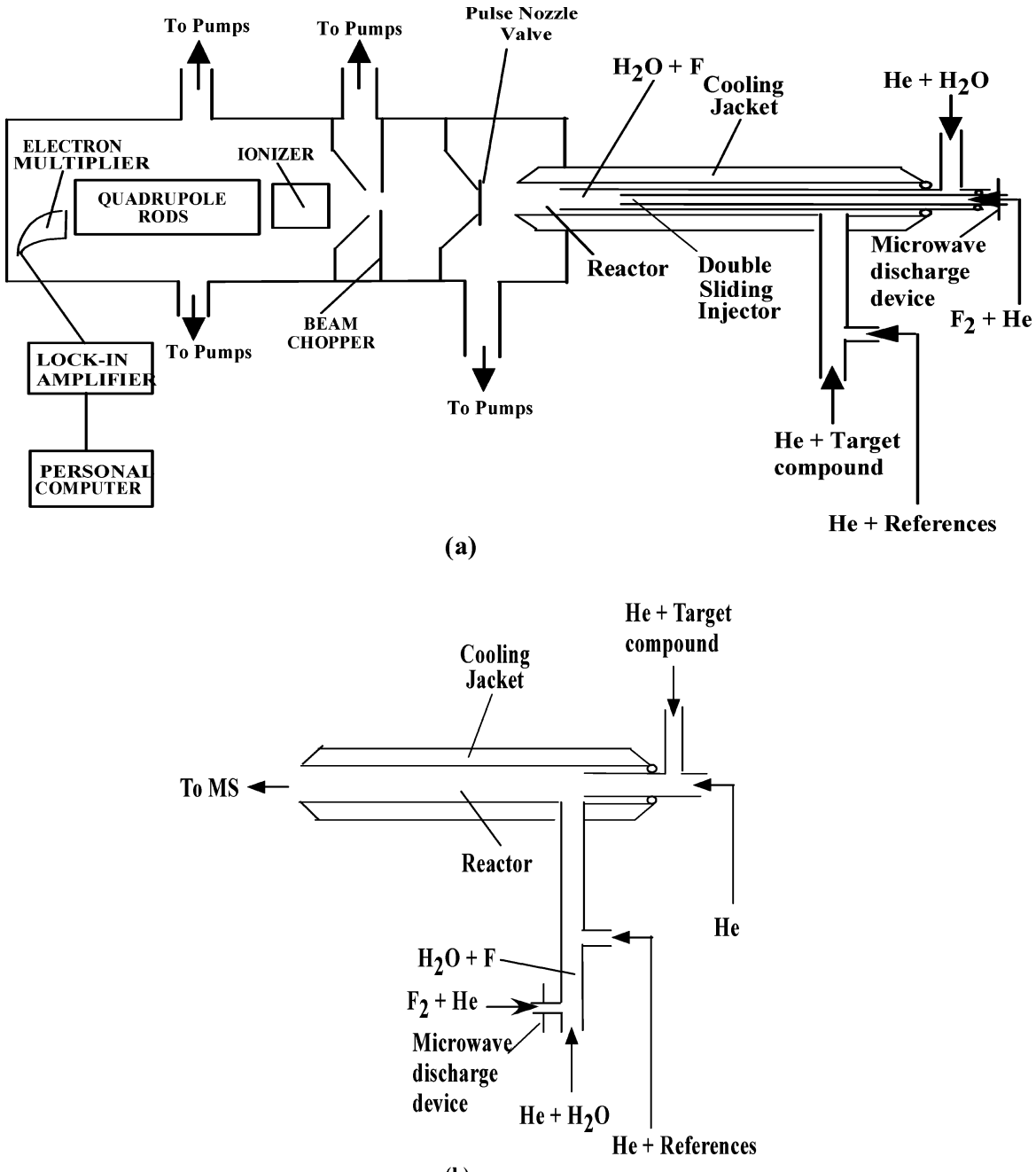

Figure 1. Experimental apparatus for RR/DF/MS study of 1,3-butadiene + OH radical reaction at 240−320 K (a) and for the controlled experiments (b). For all kinetic experiments, the F atom was produced by microwave discharge of F_2 in the sliding injector. H_2O was added through the outer sliding injector as the OH precursor. Both target and reference compounds are mixed and introduced into the reactor from sidearm.

Very little information is available in the literature regarding the products of reaction 1. In this paper, we will report our kinetics and products study of reaction 1 at 240−340 K using the relative rate/discharge flow/mass spectrometer (RR/DF/MS) technique recently developed in our laboratory.[24] We will also report our ab initio study on the reaction dynamics of reaction 1 and compare the theoretical results with the experimental observation. We will then comment on the atmospheric lifetime and atmospheric degradation of 1,3-butadiene in the atmosphere on the basis of results in the present investigation.

2. Experimental Section

The experimental apparatus used in the RR/DF/MS study of 1,3-butadiene reaction with OH radicals is shown in Figure 1, in which Figure 1a shows the arrangement for kinetics investigation and Figure 1b shows the arrangement for controlled experiments. The RR/DF/MS system has been described previously[24] and is only briefly discussed here. The flow reactor consisted of a Pyrex tube (length = 80 cm, inside diameter = 5.08 cm). The internal surface of the reactor was covered with a layer of TFE Teflon sheet (0.05 cm thick) to reduce the OH radical wall loss. A steady-state gas flow in the flow tube was achieved by using a mechanical pump (Edwards E2M175). The vacuum chamber housing the mass spectrometer was a two-stage differentially pumped vacuum system utilizing two 6-in. diffusion pumps with liquid nitrogen baffles, and the ultimate vacuum in the second stage was $<5 \times 10^{-10}$ Torr. Helium was used as a carrier gas and was introduced into the flow reactor through both a double-sliding injector and a sidearm inlet port located upstream of the reactor. A total pressure of about 1 Torr

in the flow reactor was maintained through continuous pumping during the experiments. Mean gas velocity in the flow tube was about 1200 cm s^{-1}. With an injector moving distance of 25 cm, the corresponding gaseous residence times in the reactor was about 20 ms. A removable liquid nitrogen trap was placed downstream of the reactor in order to protect the vacuum pump from corrosive reactants and products.

Mass spectrometric detection of reactants and products were carried out by continuous sampling at the downstream end of the flow tube through a two-stage beam inlet system. The mass spectrometer (Extrel Model C50) was set to emit bombarding electrons with 40 eV of impact energy. Beam modulation was accomplished with a 200-Hz tuning fork chopper placed inside the second stage of the inlets. Ion signals were sent to a lock-in amplifier (SR510) that was referenced to the chopper frequency. The amplified analogue signals were then converted to digital form (Analogue Devices RTI/815) and recorded on a microcomputer. Under normal operating conditions, the detection limit for the mass spectrometer was found to be on the order of 10^9-10^{10} molecules cm^{-3}, depending on the individual species detected.

The OH radicals were produced by the reaction of F atoms with H_2O in a double sliding injector

$$F + H_2O \rightarrow OH + HF \qquad k_2 = 1.4 \times 10^{-11}\ cm^3\ molecule^{-1}\ s^{-1}\ ^{25} \quad (2)$$

The double-sliding injector consisted of two concentric Pyrex tubes with inside diameters of 7 and 12.7 mm, respectively. The H_2O vapor was carried by 100 sccm of He to the double-sliding injector to react with the fluorine atoms generated by microwave discharge (OPTHOS INSTRUMENTS, INC. Model MPG-4) of 5% F_2 that was carried by 1500 sccm of He. The internal surface of inner Pyrex tube was coated with halocarbon wax (series 1500, Halocarbon Products Corp.) to reduce F atom loss due to reaction with SiO_2.

Both 1,3-butadiene and the reference compound (isoprene or propionaldehyde) were carried by ~100−200 sccm of He and introduced into the flow reactor from a sidearm inlet port. Prior to entering the reactor, the target and reference compounds were mixed to ensure that they shared the same reaction time with the OH radicals.

The concentration of the species in the flow reactor was determined either by flowing the known amount of sample into the reactor or by quantitative conversion of the species through chemical reactions. In particular, F atom concentration was determined by measuring the $[F_2]$ difference between "switch on" and "switch off" of the microwave discharge device, while F_2 was passing through the discharge cavity: $[F] = 2\Delta[F_2] = 2([F_2]_{\text{switch off}} - [F_2]_{\text{switch on}})$. The initial $[F_2]$ was determined by measuring the flow reactor pressure change before and after the F_2 was introduced into the reactor, which was then used to calibrate the mass spectrometer. The $[H_2O]$ was also determined from the pressure difference in the reactor before and after the H_2O was introduced. The initial concentration of the OH was taken to be nearly the same as the atomic fluorine concentration due to the quick titration of the F atoms in the double-sliding injector.

The reactor temperature was varied and controlled at 240−340 K using a temperature bath circulator (Neslab ULT-80) by circulating either methanol or water through an outer Pyrex jacket for experiments either at low ($T < 298$ K) or at high ($T \geq 298$ K) temperatures, respectively. Each temperature-dependent experiment was performed 2−4 times at different dates under the same experimental conditions to check the consistency of the experimental results.

On the basis of the theory of the RR/DF/MS technique,[24] rate constant determination for reaction 1 is briefly described as following. By assumption that 1,3-butadiene and a reference compound reacted only with OH radicals, then

$$CH_2{=}CH{-}CH{=}CH_2 + OH \rightarrow \text{products} \quad (1)$$

$$\text{reference compound} + OH \rightarrow \text{products} \quad (3)$$

It can be shown that[24]

$$\ln\frac{[\text{1,3-butadiene}]_{t,0}}{[\text{1,3-butadiene}]_{t,[OH]}} = \frac{k_1}{k_3}\ln\frac{[\text{reference}]_{t,0}}{[\text{reference}]_{t,[OH]}} \quad (I)$$

where $[\text{1,3-butadiene}]_{t,0}$ and $[\text{reference}]_{t,0}$ are the concentrations of 1,3-butadiene and the reference compound in the absence of OH radicals at time t, $[\text{1,3-butadiene}]_{t,[OH]}$ and $[\text{reference}]_{t,[OH]}$ are the concentrations of 1,3-butadiene and the reference compound in the presence of OH radicals at time t, and k_1 and k_3 are the rate constants for reactions 1 and 3, respectively. By monitoring the decay of both 1,3-butadiene and the reference compound, a straight line with a slope equal to k_1/k_3 is expected to be generated from the plot of $\ln([\text{1,3-butadiene}]_{t,0}/[\text{1,3-butadiene}]_{t,[OH]})$ vs $\ln([\text{reference}]_{t,0}/[\text{ reference}]_{t,[OH]})$. The k_1 can then be calculated if the absolute value of k_3 is known. Also if the temperature dependence of k_3 is known, repeating the above exercise at different temperatures allows determination of the temperature dependence for k_1. In the present work, experiments were carried out at a total pressure of 1−1.1 Torr in the flow reactor at 240−340 K.

During the experiments, 1,3-butadiene, isoprene, and propionaldehyde were monitored by the mass spectroscopic detection of their parent ion at m/e =54, 68, and 58, respectively. It was found that under our experimental conditions isoprene did not produce significant fragment daughter ions at $m/e = 54$ and 58 and that propionaldehyde did not produce fragment daughter ion at $m/e = 54$ in the electron impact mass spectrometer. Therefore, there was essentially very little interference in our mass spectroscopic detection of 1,3-butadiene, isoprene, and propionaldehyde parent ions, and the decay of these reactants after introducing OH into the flow reactor was considered to be primarily due to reactions of these reactants with the OH radicals.

Helium (99.999%) was obtained from Oxygen Service Company and F_2 (5% in He) from Spectra Gases, Inc. Reactants were purchased from Aldrich Chemical company, Inc.: 1,3-butadiene, >99%; isoprene, >99%; propionaldehyde, >99%. All samples were used as received. Distilled water was used as the OH precursor.

3. Theoretical Approach

All calculations were implemented using the Gaussian 98 program.[26] Reactants, products, and transition state structures involved in reaction 1 were optimized using Møller−Plesset correlation energy correction truncated at second-order (MP2) theory[26] in conjunction with 6-311++G(d,p)[26] basis set (MP2/6-311++G(d,p)). Geometry optimizations were followed by a frequency analysis using the same level of theory and basis set. All geometries were optimized to better than 0.001 Å for bond distance and 0.1° for bond angles using Schlegel's method. In addition, intrinsic reaction coordinate (IRC) calculations were carried out at the MP2/6-311++G(d,p) level to determine the minimum energy path that the transition states followed,

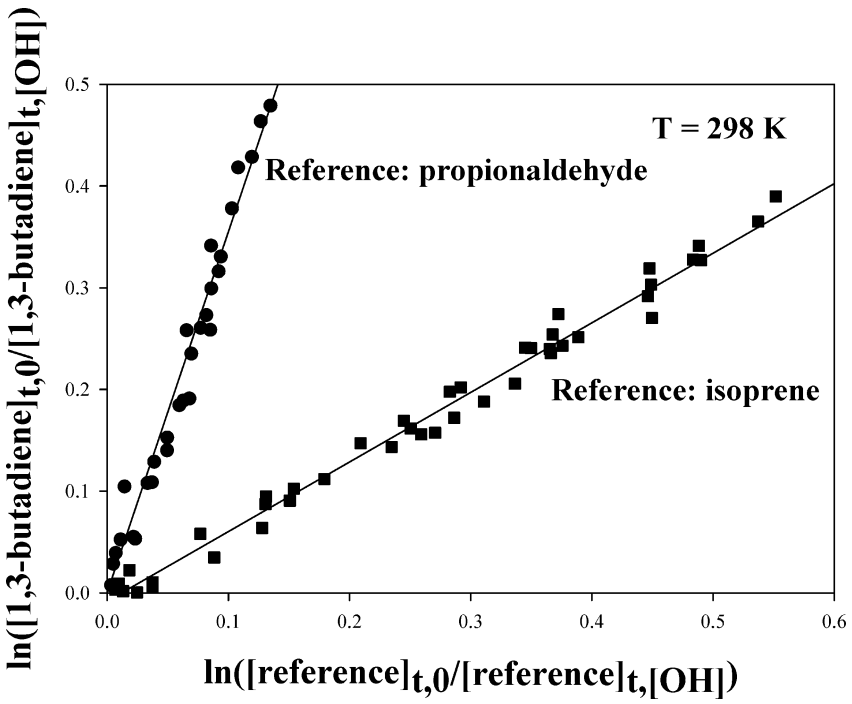

Figure 2. Typical kinetic data acquired with RR/DF/MS technique at a fixed reaction time of 20 ms for reaction of 1,3-butadiene with OH radical using isoprene and propionaldehyde as references. The experiments were carried out at 298 K and a total pressure of 1.0−1.1 Torr. Initial concentrations of 1,3-butadiene, isoprene, and propionaldehyde were about 3.8×10^{13}, 2.3×10^{13}, and 1.8×10^{13} molecules cm^{-3}, respectively. The OH concentration was varied in a range of $(0-3.5) \times 10^{13}$ molecules cm^{-3}.

connecting to appropriate reactants and products. Single-point energy calculations were performed on the involved species using Møller−Plesset perturbation theory at fourth-order (PMP4)[26] with 6-311++G(d,pd)[26] basis set using the geometry optimized at MP2/6-311++G(d,p) level. Addition of zero-point energy correction (ΔZPE) to the single-point energy, i.e., PMP4/6-311++G(d,pd)//MP2/6-311++G(d,p) + ΔZPE, was chosen to be the best estimated energy for the reactions in the present work.

4. Results and Discussion

A. Kinetics and Products. Figure 2 shows a typical kinetic data set acquired with the RR/DF/MS technique at a fixed reaction time of 20 ms for the reaction of 1,3-butadiene with OH radicals using propionaldehyde and isoprene as reference compounds. Both sets of the experimental data were collected at 298 K and a total pressure of 1−1.1 Torr. It can be seen from Figure 2 that the 1,3-butadiene decay, propionaldehyde decay, and isoprene decay followed the kinetic relationship predicted by eq I very well. Linear regression for the data in both plots produced a rate constant ratio of k_1/k_3 (propionaldehyde as reference) = 3.546 ± 0.210 and k_1/k_3 (isoprene as reference) = 0.684 ± 0.024, respectively. The recommended rate constants for the reactions of hydroxyl radical with propionaldehyde and isoprene were 1.98×10^{-11} and 9.99×10^{-11} cm^3 $molecule^{-1}$ s^{-1}, respectively.[27] The rate constants for reaction 1 were then determined to be $(7.02 \pm 0.42) \times 10^{-11}$ and $(6.83 \pm 0.24) \times 10^{-11}$ cm^3 $molecule^{-1}$ s^{-1}, respectively, which led to an average of $k_1 = (6.93 \pm 0.48) \times 10^{-11}$ cm^3 $molecule^{-1}$ s^{-1} at 298 K. The quoted error bars were taken as 2σ for this work, which took into account the scatter of data and uncertainty of the experimental parameters such as pressure, temperature, and flow rates.

It is imperative to assess the effects of possible reactions other than reactions 1 and 3 on the concentration of 1,3-butadiene and the reference compounds in order to report reliable kinetic parameters for reaction 1. In the present study, there was a concern regarding the possibility that the fluorine atom generated by the microwave discharge of F_2 might react with 1,3-butadiene and/or the reference compounds. However, since there were much more water molecules ($\sim 7.1 \times 10^{14}$ molecule cm^{-3}) than the F atoms ($\sim 3.0 \times 10^{13}$ molecule cm^{-3}) in the double-sliding injector, essentially all of the fluorine atoms should have been titrated by the water molecules in about 0.5 ms within the injector. Experimentally we checked the presence of F atoms in our chemical system by monitoring SiF_4 produced from F + SiO_2 at $m/e = 85$ when varying the amount of H_2O and observed no SiF_4 signals when $\sim 7 \times 10^{14}$ molecule cm^{-3} of H_2O was used to titrate the F atoms in the double-sliding injector. This avoided significant interaction between the fluorine atoms and any of the reactants, and hence the atomic fluorine should have contributed very little to the decay of both 1,3-butadiene and the reference compounds. Another concern regarding the accuracy of the relative rate kinetic measurements was whether the reaction products from the reactions of OH with 1,3-butadiene and the reference compound could have affected our kinetic results. To address this concern, a series of controlled experiments were conducted to examine the contribution of the reaction products to the reactant decay. The controlled experiments were designed such that the 1,3-butadiene interacted directly with the products produced from the reaction of OH with either propionaldehyde or isoprene and that either propionaldehyde or isoprene interacted directly with the product generated from the reaction of OH with 1,3-butadiene. This was achieved by rearranging the apparatus for OH generation and reactant inlets, in which the OH radicals was produced from the sidearm of the reactor followed by reacting with a reference compound while traveling through the sidearm (see Figure 1b). The products of OH + reference then entered the reactor from the sidearm port. These products then interacted with the 1,3-butadiene introduced from the sliding injector. In the case of testing if the products from 1,3-butadiene + OH would react

TABLE 1: Rate Constant Ratio, k_1/k_3, and Rate Constant, k_1 (in cm^3 molecule^{-1} s^{-1}), for 1,3-Butadiene + OH Reaction at 240−340 K[a]

temperature (K)	slope[b] (k_1/k_3)	k_1[b] ($\times 10^{11}$)	slope[c] (k_1/k_3)	k_1[c] ($\times 10^{11}$)	k_1[d] ($\times 10^{11}$)
240	0.702 ± 0.016 (29)	9.62 ± 0.22	3.487 ± 0.125 (34)	9.62 ± 0.34	9.62 ± 0.40
260	0.689 ± 0.015 (19)	8.33 ± 0.18	3.525 ± 0.264 (32)	8.53 ± 0.64	8.43 ± 0.66
277	0.676 ± 0.010 (26)	7.44 ± 0.11	3.486 ± 0.211 (44)	7.67 ± 0.46	7.56 ± 0.47
298	0.684 ± 0.024 (36)	6.83 ± 0.24	3.546 ± 0.210 (45)	7.02 ± 0.42	6.93 ± 0.48
320	0.675 ± 0.021 (18)	6.16 ± 0.19	3.412 ± 0.148 (40)	6.18 ± 0.27	6.17 ± 0.33
340	0.668 ± 0.019 (27)	5.68 ± 0.16	3.280 ± 0.168 (33)	5.51 ± 0.28	5.60 ± 0.32

[a] Note: Error bars are taken as 2σ. The numbers in parentheses represent data points collected. [b] By use of propionaldehyde as reference. [c] By use of isoprene as reference. [d] Average of the measured rate constants using isoprene and propionaldehyde as references.

TABLE 2: Reaction Scheme for Chemical Model Simulation in RR/DF/MS Kinetic Data Analysis

reaction[a]	k (cm^3 molecule^{-1} s^{-1})	ref
$F + H_2O \rightarrow HF + OH$	1.4×10^{-11}	25
$OH + OH \rightarrow H_2O + O$	1.9×10^{-12}	25
OH + wall → product	10[b]	estimate[d]
$O + OH \rightarrow O_2 + H$	3.3×10^{-11}	25
H + wall → product	10[b]	estimate[d]
$H + OH + M \rightarrow H_2O + M$	2.3×10^{-31}[c]	27
$O + F_2 \rightarrow FO + F$	1.0×10^{-16}	27
$FO + OH \rightarrow O_2 + HF$	1.3×10^{-12}	estimate[e]
$H + F_2 \rightarrow HF + F$	1.38×10^{-12}	27
C_2H_5CHO[f] $+ OH \rightarrow H_2O + C_2H_5CO$	2.0×10^{-11}[f]	27
C_4H_6(1,3-butadiene) + OH → products	6.95×10^{-11}	this work
$C_2H_5CHO + O \rightarrow OH$ + other products	7.1×10^{-13}[g]	27
$C_4H_6 + O \rightarrow$ product	1.7×10^{-11}	27
$C_2H_5CHO + H \rightarrow H_2 + C_2H_5CO$	1.2×10^{-13}[h]	27
$C_4H_6 + H \rightarrow$ products	8.34×10^{-12}	27

[a] Initial concentrations are: $[F]_0 = 3.0 \times 10^{13}$, $[H_2O]_0 = 7.1 \times 10^{14}$, $[F_2]_0 = 2.0 \times 10^{12}$, $[C_4H_6]_0 = 3.8 \times 10^{13}$, $[C_2H_5CHO]_0 = 1.8 \times 10^{13}$, and $[\text{isoprene}]_0 = 2.3 \times 10^{13}$ molecule cm^{-3}, respectively. The initial concentrations of all other species are set to be zero. [b] The unit is s^{-1} for the wall-loss process. [c] the unit is cm^6 molecule^{-2} s^{-1}. [d] Estimate based on OH wall loss. [e] Estimate based on k(ClO + OH). [f] When isoprene is used as a reference, $k = 9.5 \times 10^{-11}$ cm^3 molecule^{-1} s^{-1} for isoprene + OH at 298 K. [g] $k = 3.5 \times 10^{-11}$ cm^3 molecule^{-1} s^{-1} for isoprene + O at 298 K. [h] $k = 8.34 \times 10^{-12}$ cm^3 molecule^{-1} s^{-1} is estimated for isoprene + H at 298 K based on $k(C_4H_6 + H)$.

with the reference compound, the inlets of the organics were swapped. About 1.5×10^{13} molecule of 1,3-butadiene was in contact with the products from the reaction of $\sim 1.2 \times 10^{13}$ molecule of OH with $(1.3-2.2) \times 10^{13}$ molecule of propionaldehyde or isoprene in our controlled experiments. It was found that the products from OH + propionaldehyde or isoprene had little effect on the 1,3-butadiene mass spectral signal intensity. Likewise, the products from the OH + 1,3-butadiene reaction had little effects on the propionaldehyde or isoprene mass spectral intensity. Finally, the effect of reactions of 1,3-butadiene and references with atomic oxygen generated from the OH self-reaction on our kinetics results was also assessed using a chemical model which utilized the Runge−Kutta method to numerically solve differential equations of our chemical system and calculated the concentration of chemical species of interest in the system as a function of time.[24] Table 2 lists the reactions that are used in our modeling along with necessary parameters such as rate constants and initial concentration of the major reactants. Our model predicted that the concentrations of the O atoms be less than 1.3×10^{11} and 7.0×10^{10} molecule cm^{-3} in our chemical system when propanal and isoprene were used as reference compounds and the oxygen atoms caused less than 1% decay of the 1,3-butadiene and references during 50 ms under our experimental conditions. This indicated that the decay of both 1,3-butadiene and the reference compounds was mainly due to their reaction with the hydroxyl radicals, and our kinetics data acquired using the RR/DF/MS technique should not be affected by the reaction products. In fact, within experimental uncertainty, our k_1 value of $(6.93 \pm 0.48) \times 10^{-11}$ cm^3 molecule^{-1} s^{-1} at 298 K is in very good agreement with $k_1 = (6.85 \pm 0.69) \times 10^{-11}$, $(6.66 \pm 0.20) \times 10^{-11}$, and $(7.71 \pm 1.54) \times 10^{-11}$ cm^3 molecule^{-1} s^{-1} reported by Atkinson et al.,[21] Atkinson and Aschmann,[28] and Lloyd et al.[29] using different techniques.

The rate constant for reaction 1 was also determined at 240, 260, 277, 320, and 340 K using the RR/DF/MS technique, and the results are also given in Table 1. Figure 3 shows our Arrhenius plot for reaction 1 along with the available experimental data at 299−424 K in the literature. It can be seen from Figure 3 that our data at $T = 298-340$ K are in very good agreement with that determined by Atkinson et al.[21] and by Liu et al.[22] at 299−424 K, within experimental uncertainty. Thus an extension of our temperature-dependent study to lower temperatures preserved a trend that the rate constant for the reaction 1 increased with decreasing temperature. This suggests that the rate constant of reaction 1 is negatively dependent on temperature at 240−340 K. Fitting our data points into a straight line yielded an Arrhenius expression for reaction 1 to be $k_1 = (1.58 \pm 0.07) \times 10^{-11} \exp[(436 \pm 13)/T]$ cm^3 molecule^{-1} s^{-1}, in which the error bars were also taken as 2σ. Our result of temperature dependence of the rate constant for reaction 1 is also in excellent agreement with that reported by Atkinson et al.[21] and Liu et al.[22] in which the Arrhenius expression for reaction 1 was determined to be $k_1 = 1.45 \times 10^{-11} \exp[(468 \pm 151)/T]$ cm^3 molecule^{-1} s^{-1} and $k_1 = (1.4 \pm 0.1) \times 10^{-11} \exp[(440 \pm 40)/T]$ cm^3 molecule^{-1} s^{-1}, respectively.

There was a concern about using isoprene as a reference compound for the kinetics investigation of reaction 1 under at ca. 1 Torr since the rate constant for the OH + isoprene may be in the falloff region between 280 and 340 K.[30,31] If the OH reaction with isoprene had a strong pressure dependence at low pressure, there would be a question about the accuracy of our rate constant measurement for the reaction using isoprene as a reference compound, especially at $T \geq 298$ K. To address this question, a separate kinetic study of the OH + isoprene reaction was conducted in our laboratory using the RR/DF/MS method. The experiments were carried out at 298−340 K and a total pressure of 1 Torr using both 1,4-dioxane and propionaldehyde as reference compounds. Our preliminary results suggested that, within the experimental uncertainty, the rate constant of OH + isoprene determined at 1 Torr was not significantly different from that reported at higher pressures in the literature, and at 298, 320, and 340 K the rate constant values were found to be 4−7% smaller than those recommended by the IUPAC subcommittee.[27] Therefore, the rate constant of OH + 1,3-butadiene determined using isoprene as a reference compound in the present work should be reliable. The fact that our Arrhenius expression is consistent with those reported at high-pressure limits indicated that the falloff region of reaction 1 may be below 1 Torr.

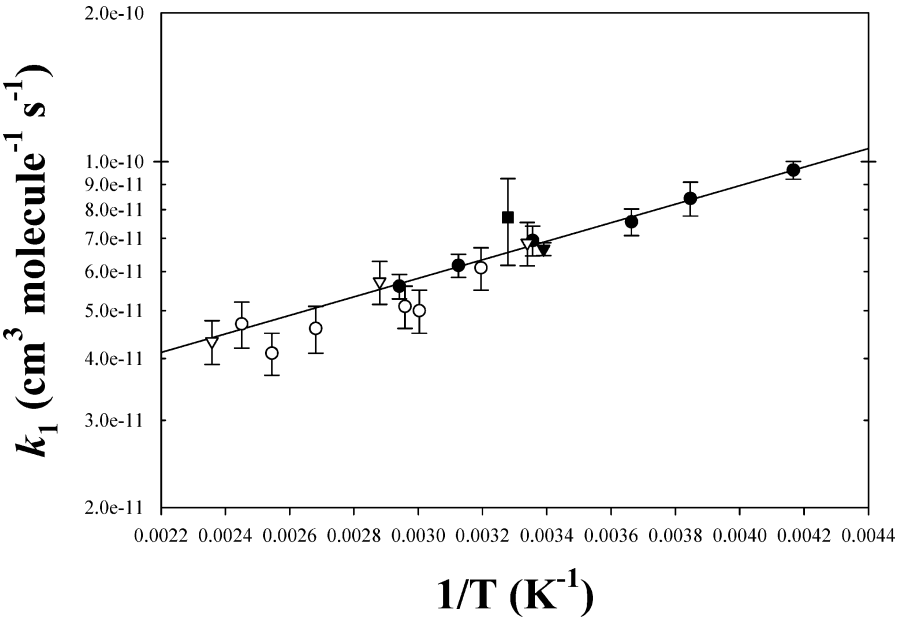

Figure 3. Arrhenius plot of 1,3-butadiene + OH: filled circle, this work; filled triangle, ref 28; open triangle, ref 21; open circle, ref 22; filled square, ref 29. Linear fitting of the data set of the present work yielded an Arrhenius expression of $k_1 = (1.58 \pm 0.07) \times 10^{-11} \exp[(436 \pm 13)/T]$ cm^3 molecule^{-1} s^{-1} at 240−340 K for the reaction.

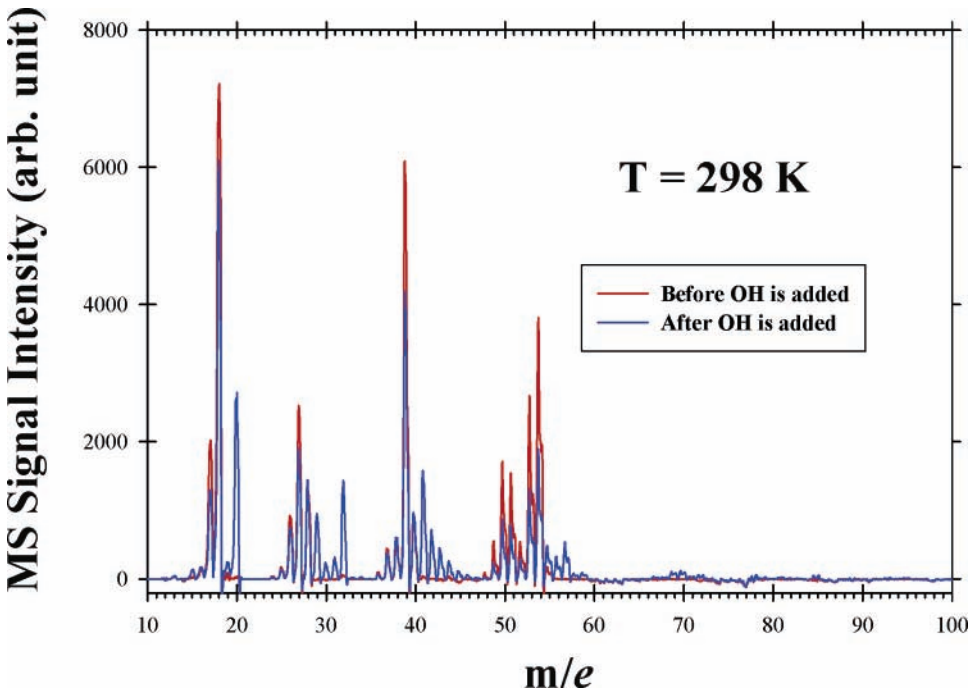

Figure 4. Mass spectra for the OH + 1,3-butadiene system at 298 K and a total pressure of 1.1 Torr. The red line profile represents the mass spectrum taken before OH was introduced into the reactor, and the blue line profile represents the mass spectrum collected after OH was added to the reactor. The initial concentrations of 1,3-butadiene and OH were about 7.5×10^{13} and 5.0×10^{13} molecule cm^{-3}, respectively.

The products from the reaction of 1,3-butadiene with OH were also studied in the present work using mass spectrometry, and Figure 4 shows the mass spectrum of 1,3-butadiene before and after reacting with the OH radicals. Major product peaks are found at m/e = 70, 69, 59−55, 45−40, 32−28, and 20. This observation is consistent with the results of Peeters et al.[32] using 30 eV of electron impact energy. No evidence was found for the hydrogen abstraction by the OH radical since the peak at m/e = 53 decreased after reaction 1 took place. The peak at m/e = 20 is assigned to the HF^+ ion due to reaction of atomic fluorine with water. On the basis of reactions 1.1 and 1.2, the peaks at m/e = 70 and 69 are assigned to the daughter ions of either $C(OH)H_2$—•CH−CH═CH_2 or •CH_2—C(OH)H—CH═CH_2, respectively. The peak at m/e = 57 is assigned to C(OH)H—CH═CH_2^+, which is most likely resulted from C1—C2 bond rupture of •CH_2—C(OH)H—CH═CH_2 other than the C3—C4 bond rupture of CH_2(OH)—•CH—CH═CH_2 based on our computational results (see discussion in section B). The peaks at m/e = 44−41 are assigned to either $C(OH)H_2$—CH^+ or CH_2—$C(OH)H^+$ and their daughter ions, which can be generated from the breakage of C2−C3 bond in $C(OH)H_2$—• CH—CH═CH_2 and •CH_2—C(OH)H—CH═CH_2, respectively. The peak at m/e = 40 is assigned to CH—CH═CH_2^+, which could be exclusively yielded from rupture of C1—C2 bond in $C(OH)H_2$—CH•—CH═CH_2. Finally, the peaks at m/e = 31−28 are assigned to $C(OH)H_2^+$ and its daughter ions. We are

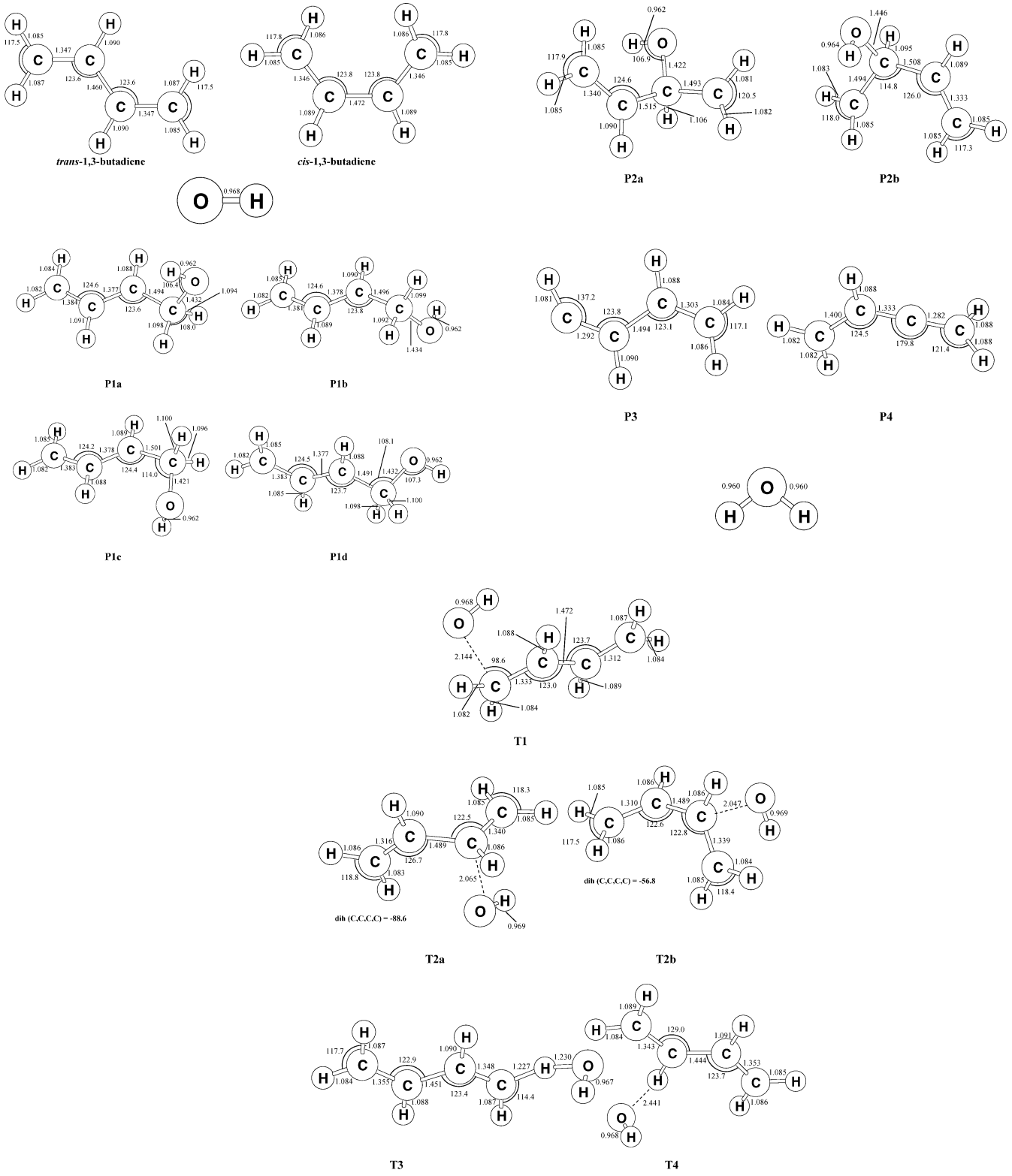

Figure 5. Optimized geometry of reactants, products, and transition states for the reaction of OH with 1,3-butadiene. All optimizations are calculated at MP2/6-311++G(d,p) level of theory. The bond lengths are in angstroms, and angles are in degrees.

currently unable to assign peaks at $m/e = 32$, 45, 58, and 59 using the chemical scheme of reactions 1.1−1.4. These species could be due to the isomerization of the primary reaction products followed by fragmentation during their ionization.[32] On the basis of the analysis above, combination of peaks at $m/e = 40$ and 31−28 implies the addition of OH radical to the terminal carbon of the 1,3-butadiene molecule. Further atmospheric oxidative degradation of the $C(OH)H_2-CH\bullet-CH=CH_2$ radical has been found to lead to formation of acrolein, formaldehyde, and unsaturated hydrocarbonyl.[23] The observation of peak at $m/e = 57$ provides an evidence of addition of OH to the internal carbon of 1,3-butadiene, through either primary reaction or secondary reactions. Tuazon et al.[23] and Liu et al.[9] had examined the products formed from the reaction of OH radical with 1,3-butadiene in a Teflon chamber with presence of O_2 and NO, and they suggested that the observed furan and maloaldehyde were likely to be produced from the subsequent reaction of $\bullet OOCH_2CH(OH)CH=CH_2$, which could only be

TABLE 3: Total Energy and ZPE (in Hartree) of the Species Involved in the OH + 1,3-Butadiene System

species	MP2/ 6-311++G(d,p)	PMP4/ 6-311++G(d,pd)	ZPE[a]
trans-1,3-butadiene	−155.52691	−155.61548	0.08439
cis-1,3-butadiene	−155.52305	−155.61169	0.08508
OH	−75.57991	−75.60189	0.00874
H_2O	−76.27492	−76.29828	0.02169
T1	−231.08927	−231.22162	0.09851
T2a	−231.08752	−231.21111	0.10077
T2b	−231.08873	−231.21344	0.10065
T3	−231.08713	−231.20519	0.09182
T4	−231.09130	−231.20895	0.09141
P1a	−231.16527	−231.28358	0.10128
P1b	−231.16290	−231.28150	0.10089
P1c	−231.16377	−231.28212	0.10112
P1d	−231.16327	−231.28164	0.10095
P2a	−231.14974	−231.25743	0.10198
P2b	−231.15013	−231.25742	0.10051

[a] ZPE computed at the MP2/6-311++G(d,p) level of theory.

derived from the addition of OH to the internal carbon of 1,3-butadiene. Our observation of the evidence of OH attack on the internal carbon of 1,3-butadiene supports their postulation. However, it is unclear whether the terminal carbon attack or the internal carbon attack is preferred as the primary process of reaction 1, since our instrument was unable to make such a determination. Therefore further investigations are required to address this question.

B. Ab Initio Study of the Reaction Pathways of Reaction 1. To better understand the reaction of OH with 1,3-butadiene, ab initio molecular orbital calculations were carried out to investigate the chemical dynamics of this reaction. Figure 5 shows the molecular configurations of the reactants, products, and transition state complexes optimized at the MP2/6-311++G(d,p) level of theory for the OH + 1,3-butadiene chemical system. Corresponding total energy, ZPE values for each of these species are given in Table 3 and frequencies in Table 4, respectively. All stable reactant and product species were found to have frequencies that were positive, indicating a minimum on the potential surface for each of these species. All transition state complexes were found to have one imaginary frequency along the reaction path connecting to appropriate reactants and products on the potential surface, which was confirmed by the IRC calculations. Relative energy of products and transition state complexes referenced to the reactants is given in Table 5. Our computational results predicted that there are two configurations for 1,3-butadiene, namely, *trans*-1,3-butadiene and *cis*-1,3-butadiene, as shown in Figure 5, with *trans*-1,3-butadiene being 2.8 kcal mol^{-1} more stable than its cis isomer at PMP4/6-311++G(d,pd)//MP2/6-311++G(d,p) + ΔZPE level of theory (Table 5). The bond lengths of the C1−C2 and C3−C4 bonds are predicted to be 1.347 Å for *trans*-1,3-butadiene and 1.346 Å for *cis*-1,3-butadiene, respectively, which indicates a double-bond feature for these carbon−carbon bonds. The bond length of the C2−C3 bond is calculated to be 1.460 and 1.472 Å for *trans*- and *cis*-1,3-butadiene, respectively, and the longer C2−C3 bond in *cis*-1,3-butadiene may be due to the repulsion between the hydrogen atoms attached to C2 and C3. The −C−C−C angles are predicted to be 123.6 and 123.8° for *trans*-1,3-butadiene and *cis*-1,3-butadiene, respectively. The C1−C2 bond, C2−C3 bond, and the −C−C−C angle of *trans*-1,3-butadiene have been experimentally determined to be 1.337 Å, 1.476 Å, and 122.9°, respectively,[33] and with a difference of about 1% or less our calculated structural values for the *trans*-1,3-butadiene agrees very well with these experimental values. This indicates that the MP2/6-311++G(d,p) level of theory is appropriate to describe the structural parameters for the chemistry involving 1,3-butadiene.

Four stable adduct products (**P1a**, **P1b**, **P1c**, and **P1d**) were located for the addition of the OH radical to the C1 atom, with **P1a** the most stable form of these isomers, and we believe that the adducts **P1b**, **P1c**, and **P1d** resulted from the rotation of the $-CH_2OH$ group along the C1−C2 bond. Our computational results also suggest a 1.421−1.434 Å length for the C−O bond, and a 1.491−1.501 Å length for the C1−C2 bond of the **P1** adducts, revealing a change of the C1−C2 bond from a double-bond to a single-bond feature. The C2−C3 and C3−C4 bonds are computed to be in the range of 1.377−1.384 Å, which reveals a double-bond feature, suggesting a delocalization of the π electron among the C2, C3, and C4 carbon atoms. The substantially longer C1−C2 bond than C2−C3 and C3−C4 bonds suggests that the C1−C2 bond is much weaker than the C3−C4 bond and hence the rupture of C1−C2 bond is more favorable over the C3−C4 bond cleavage during the ionization of the **P1** adducts.

The addition of OH to the C2 atom was predicted to form an adduct (**P2a** or **P2b**) that increases the C1−C2 and C2−C3 bond lengths of both *trans*- and *cis*-1,3-butadiene by ca. 0.16 Å and hence weakening these bonds. As a result, both the C1−C2 and C2−C3 bonds are more likely to be broken than the C3−C4 bond, giving rise to our observation of fragmentation ion peaks at $m/e = 57$ and 44, respectively, when they are ionized by electron bombardment. In the case of *cis*-1,3-butadiene, the adduct **P2b** is expected to possess a smaller C1−C2−C3 angle and a slightly larger C2−C3−C4 angle compared to *cis*-1,3-butadiene based on our calculation results.

The product formed from the abstraction of a hydrogen atom from C1 (**P3**) is found to be associated with a decrease of the C1−C2 and C3−C4 bond lengths by ca. 0.05 Å and an increase in the C2−C3 bond by 0.03 Å of the *trans*-1,3-butadiene. However, when the hydrogen atom on C2 is abstracted, the product is expected to change significantly in structure (**P4**) and the C1−C2 and C2−C3 bond lengths are predicted to decrease by 0.065 and 0.127 Å, respectively. Moreover, the C1, C2, and C3 atoms are anticipated to be essentially positioned in a straight line.

Transition state complexes for reactions 1.1−1.4 were located in the present work at the MP2/6-311++G(p,d) level of theory. These transition states were confirmed by IRC calculations indicating their connection to corresponding reactants and products. The transition state for the addition of OH to C1 of *trans*-1,3-butadiene (**T1**) and C2 of both *trans*- and *cis*-1,3-butadiene (**T2a** and **T2b**) are predicted to have a C−O bond greater than 2.04 Å, indicating a reactant-like transition state complex for these processes. The transition state structure for abstraction of hydrogen atom from C2 (**T4**) is also suggested to be reactant-like since the O−H bond is calculated to be 2.441 Å. However, the transition state structure for the abstraction of a hydrogen atom from C1 is found to share a similar C1−H and O−H bond length, while the other structural parameters experiences only minor changes (**T3**).

Figure 6 summarizes the data of Table 5 showing our best estimate for the relative energy of reaction 1 based on single point calculation at MP4/6-311++G(d,pd) level of theory plus ZPE correction (PMP4/6-311++G(d,pd) + ΔZPE). Our best energetic estimate suggests that both the addition of OH to 1,3-butadiene and the abstraction of hydrogen atoms from 1,3-butadiene by the OH radical are exothermic processes. At the PMP4/6-311++G(d,pd) + ΔZPE level of theory, our calculation predicts a reaction energy barrier of 0.7 and 8.7 kcal mol^{-1}

TABLE 4: Vibrational Frequency Calculated at the MP2/6-311++G(d,p) Level of Theory for Various Species Involved in the OH + 1,3-Butadiene System

species	vibrational frequencies (in cm^{-1})
OH	3837
trans-1,3-butadiene	129, 294, 506, 514, 698, 815, 816, 905, 966, 1000, 1028, 1234, 1312, 1316, 1418, 1482, 1635, 1701, 3172, 3175, 3183, 3186, 3278, 3279
cis-1,3-butadiene	190, 275, 458, 624, 744, 897, 898, 906, 997, 1020, 1068, 1098, 1303, 1333, 1439, 1474, 1669, 1670, 3174, 3177, 3183, 3193, 3278, 3280
H_2O	1629, 3885, 4003
P1a	87, 182, 275, 366, 444, 510, 552, 744, 795, 922, 991, 1031, 1051, 1133, 1166, 1213, 1310, 1332, 1391, 1432, 1507, 1518, 1535, 3060, 3134, 3184, 3200, 3206, 3313, 3875
P1b	45, 171, 228, 311, 427, 517, 557, 750, 786, 929, 987, 1027, 1038, 1118, 1145, 1225, 1314, 1364, 1373, 1431, 1505, 1518, 1536, 3051, 3157, 3183, 3193, 3201, 3312, 3884
P1c	99, 188, 223, 378, 402, 547, 661, 727, 753, 894, 987, 1021, 1042, 124, 1160, 1208, 1311, 1343, 1392, 1430, 1505, 1517, 1534, 3042, 3103, 3195, 3201, 3210, 3310, 3876
P1d	86, 180, 249, 289, 441, 507, 556, 747, 792, 927, 998, 1031, 1056, 1136, 1162, 1244, 1283, 1313, 1363, 1454, 1515, 1525, 1540, 3031, 3088, 3188, 3201, 3213, 3312, 3885
P2a	125, 198, 293, 317, 353, 436, 552, 605, 783, 904, 923, 1017, 1021, 1083, 1146, 1241, 1275, 1308, 1377, 1447, 1460, 1474, 1690, 2994, 3179, 3195, 3216, 3286, 3347, 3873
P2b	97, 199, 300, 327, 380, 400, 532, 632, 713, 848, 954,1010, 1029, 1060, 1074, 1184, 1248, 1345, 1389, 1423, 1471, 1494, 2468, 3114, 3183, 3194, 3242, 3281, 3314, 3851
P3	68, 295, 495, 608, 849, 875, 954, 999, 1030, 1145, 1169, 1268, 1351, 1474, 1697, 1902, 3180, 3190, 3216, 3288, 3298
P4	240, 269, 492, 597, 649, 673, 965, 970, 1000, 1011, 1084, 1198, 1383, 1474, 1507, 2220, 3163, 3211, 3216, 3241, 3331
T1	452*i*, 75, 91, 176, 242, 300, 524, 617, 695, 846, 914,1007, 1018, 1022, 1070, 1140, 1223, 1327, 1341, 1449, 1482, 1630, 1804, 3188, 3199, 3209, 3216, 3291, 3321, 3827
T2a	554*i*, 45,120, 228, 265, 360, 467, 679, 740, 763, 892, 980, 1046, 1083, 1106, 1112, 1130, 1322, 1358, 1449, 1481, 1677, 2642, 3181, 3193, 3229, 3260, 3303, 3309, 3813
T2b	571*i*, 108, 143, 220, 250, 369, 476, 671, 761, 771, 903, 979, 1065, 1094, 1100, 1132, 1154, 1317, 1342, 1455, 1488, 1670, 2431, 3195, 3199, 3230, 3251, 3284, 3306, 3815
T3	1905*i*, 93, 121, 160, 176, 296, 427, 548, 615, 733, 823, 878, 919, 951, 983, 1012, 1234, 1255, 1290, 1343, 1403, 1476, 1546, 2107, 3178, 3186, 3195, 3222, 3284, 3849
T4	1878*i*, 108, 141, 185, 198, 284, 453, 530, 639, 710, 812, 855, 865, 923, 978, 990, 1165, 1249, 1323, 1363, 1406, 1474, 1570, 1974, 3162, 3167, 3192, 3276, 3291, 3838

TABLE 5: Computed Relative Energy (in kcal mol^{-1}) for Reaction of OH with 1,3-Butadiene

reaction	MP2/ 6-311++ G(d,p)	PMP4/ 6-311++ G(d,pd) + ΔZPE
trans-1,3-butadiene + OH	0.0	0.0
trans-1,3-butadiene → *cis*-1,3-butadiene	2.9	2.8
trans-1,3-butadiene + OH → **T1**	14.4	0.7
trans-1,3-butadiene + OH → **T2a**	16.9	8.7
cis-1,3-butadiene + OH → **T2b**	16.1	7.2
trans-1,3-butadiene + OH → **T3**	11.5	6.8
trans-1,3-butadiene + OH → **T4**	8.7	4.2
trans-1,3-butadiene + OH → **P1a**	−31.6	−36.4
trans-1,3-butadiene + OH → **P1b**	−30.3	−35.4
trans-1,3-butadiene + OH → **P1c**	−30.7	−35.6
trans-1,3-butadiene + OH → **P1d**	−30.5	−35.4
trans-1,3-butadiene + OH → **P2a**	−22.5	−18.8
cis-1,3-butadiene + OH → **P2b**	−21.4	−19.6
trans-1,3-butadiene + OH → **P3** + H_2O	−6.8	−15.7
trans-1,3-butadiene + OH → **P4** + H_2O	−21.1	−29.3

for the addition of OH to the terminal and internal carbon of *trans*-1,3-butadiene, respectively. The activation energy for the abstraction of a hydrogen atom from the terminal and the internal carbon of *trans*-1,3-butadiene is calculated to be 6.8 and 4.2 kcal mol^{-1}, respectively. This suggests that the addition of OH to the terminal carbon of 1,3-butadiene is the most energetically favored reaction pathway due to combination of low activation energy barrier and high exothermicity. By consideration of an uncertainty of ±1 kcal mol^{-1} in our estimate for the relative energy, this reaction pathway could be a very low barrier or a barrierless process, which is consistent with the observation of the rate constant negatively dependent on temperature for reaction 1 in the present and previous studies.[21,22] A branching ratio assessment of reaction 1 using transition state theory[34] suggests that reaction 1.1 is a dominant pathway, and the addition of the OH to the internal carbon of the *trans*-1,3-butadiene and *cis*-1,3-butadiene is expected to be the most minor process. This computational result, on the other hand, is in contrast to the experimental observation of the evidence of OH addition to internal carbon in our mass spectrum of OH + 1,3-butadiene. If the theoretical prediction is correct, the peak at $m/e = 57$ in Figure 4 might be due to a secondary reaction such as isomerization of **P1**. However, since the **P1** adducts are about 16 kcal mol^{-1} more stable than the **P2a** adduct, the isomerization of **P1** adducts into **P2a** seems unlikely in the time scale of milliseconds under our experimental conditions due to this large endothermicity of the isomerization. On the other hand, there might be a different reaction pathway leading to the production of **P2a** from OH + 1,3-butadiene without involving **T2a** as a transition state. One such possible pathway could be the formation of a pre-reactive van der Waals complex followed by a transition state that has an activation energy barrier lower than the reactants. The existence of the pre-reactive van der Waal complex has been predicted for the reaction of the OH radicals with propene, an analogue of 1,3-butadiene, leading to the addition of the OH radical to the central carbon atom of the propene.[37] Further investigation is needed to resolve this contrast.

4. Summary

The kinetics of the reaction of OH with 1,3-butadiene has been investigated in the temperature range of 240−340 K using the RR/DF/MS method. At 298 K, the rate constant for this reaction was determined to be $k_1 = (6.93 \pm 0.48) \times 10^{-11}$ cm^3 $molecule^{-1}$ s^{-1}. The Arrhenius expression for this reaction was determined to be $k_1 = (1.58 \pm 0.07) \times 10^{-11} \exp[436 \pm 13/T]$ cm^3 $molecule^{-1}$ s^{-1} at 240−340 K, which was in excellent

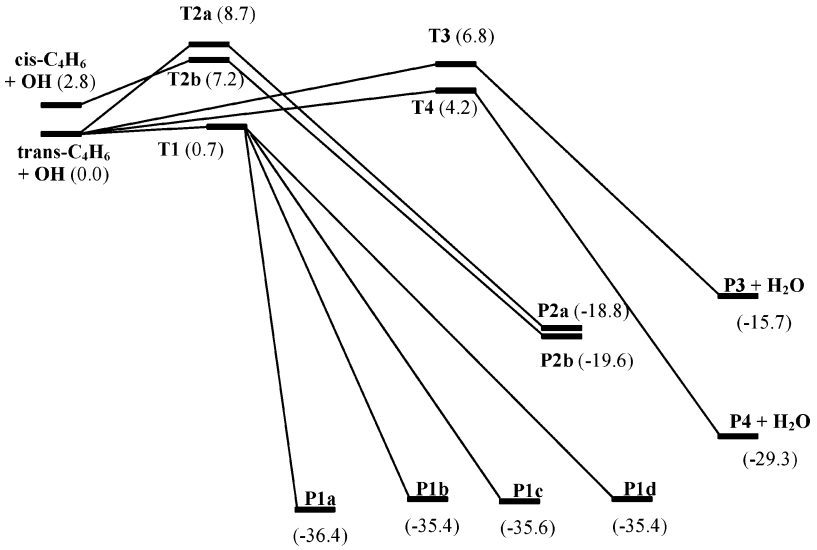

Figure 6. Calculated relative energetics (in kcal mol^{-1}) for the reaction of OH with 1,3-butadiene. The best estimate of the relative energetics is based on a single-point calculation at the PMP4/6-311++G(dp,d) level of theory plus ZPE correction using the geometry optimized at the MP2/6-311++G(d,p) level of theory.

agreement with those reported by Atkinson et al.[21] and Liu et al.[22] This agreement suggests that the rate constant of OH + 1,3-butadiene has reached a high-pressure limit at 1 Torr and that the falloff region may be below 1 Torr. Evidence was observed for the addition of OH radical to both the terminal and internal carbons of the 1,3-butadiene for reaction 1. However, it was unclear if the addition of OH to the internal carbon occurred as a primary elementary process. Our ab initio study of reaction mechanism of the OH + 1,3-butadiene system suggests that the reaction of OH with 1,3-butadiene is exothermic in reaction pathways involving either hydrogen abstraction or adduct formation, and the addition of OH to the terminal carbon atom is expected to be the most energetically favored pathway, which could be an energy barrierless process. This is consistent, within computational uncertainty, with the results of negative temperature dependence of the rate constant for this reaction. The predicted increasing C1−C2 bond length due to the addition of OH to the internal carbon atom of the 1,3-butadiene suggests a likely cleavage of this carbon−carbon bond when the adduct is ionized with an electron impact ionization source, giving rise to the observation of the C(OH)H−CH=CH_2^+ ion peak at $m/e = 57$ in the mass spectrum of OH + 1,3-butadiene.

As an approximation with the assumption that 1,3-butadiene is removed from the troposphere mainly by OH attack, the atmospheric lifetime of this compound can be assessed using the following equation[35]

$$\tau_{1,3-\text{butadiene}} = [k_{277K}(CH_3CCl_3 + \text{OH})/k_{277K}(1,3\text{-butadiene} + \text{OH})]\tau_{CH_3CCl_3} \quad (1)$$

where $k_{277K}(CH_3CCl_3 + OH) = 6.62 \times 10^{-15}$ cm^3 molecule^{-1} s^{-1} [25] and k_{277K}(1,3-butadiene + OH) are the rate constants for the reaction of methyl chloroform (CH_3CCl_3) and 1,3-butadiene with OH at 277 K, a typical average temperature of the troposphere, and $\tau_{CH_3CCl_3}$ is the atmospheric lifetime of methyl chloroform, which is 5.9 years assuming a 24-h average OH radical concentration of $(8.1 \pm 0.9) \times 10^5$ molecule cm^{-3}.[35] This leads to an atmospheric lifetime of ca. 4.5 h for the 1,3-butadiene due to OH attack. This value should be considered as an upper limit since 1,3-butadiene also reacts with other atmospheric species such as NO_3, O_3, and Cl,[36] which further decrease the atmospheric lifetime of this molecule. Finally, our product study of reaction 1 suggests that the formation of adduct is the dominant pathway for reaction 1. While it is unclear if the OH addition to the internal carbon of 1,3-butadiene is a primary chemical process, the fact that the OH radical may add to the internal carbon of 1,3-butadiene provides mechanistic evidence for the possible formation of furan and maloaldehyde in the atmosphere:[9,23]

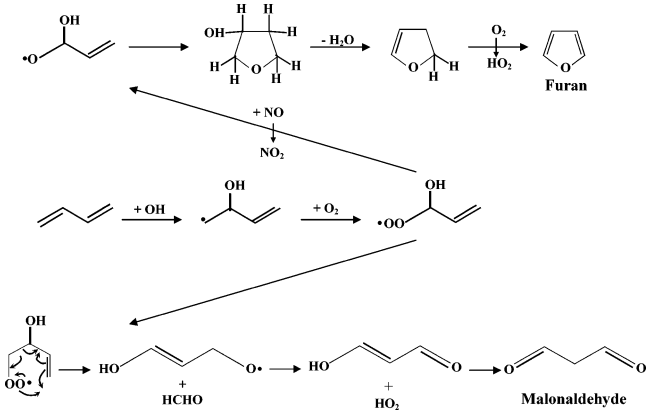

Further studies are needed regarding the subsequent degradation of these compounds in the atmosphere to complete our understanding of the role of 1,3-butadiene in the air pollution system.

Acknowledgment. This work was supported in part by the National Science Foundation (NSF ATM-0533574), the CSU Special Fund for Research, Scholarship, and Creative Activity Minigrant, and the Untenured Faculty Support Grants of CSUF. H.K.L. thanks the support from NSFC(20333050).

References and Notes

(1) U.S. Department of Labor—Occupational Safety & Health Administration. 30 December 2002. http://www.osha.gov/SLTC/butadiene/, December 2004.

(2) Eatough, D. J.; Hansen, L. D.; Lewis, E. A. *Environ. Technol.* **1990**, *11*, 1071.

(3) Kirchstetter, T. W.; Singer, B. C.; Harley, B. A. *Environ. Sci. Technol.* **1996**, *30*, 661.
(4) Hoekman, S. K. *Environ. Sci. Technol.* **1992**, *26*, 1206.
(5) Boudries, H.; Toupance, G.; Dutot, A. L. *Atmos. Environ.* **1994**, *28*, 1095.
(6) Mowrer, J.; Lindskog, A. *Atmos. Environ.* **1991**, *25A*, 1971.
(7) Grosjean, E.; Grosjean, D.; Rasmussen, R. A. *Environ. Sci. Technol.* **1998**, *32*, 2061.
(8) Löfgren, L.; Petersson, G. *Sci. Total Environ.* **1992**, *116*, 195.
(9) Liu, X.; Jeffries, H. E.; Sexton, K. G. *Atmos. Environ.* **1999**, *33*, 3005.
(10) California Environmental Protection Agency's Air Resources Board and Office of Environmental Health Hazard Assessment, May 1992. http://www.oehha.ca.gov/air/toxic_contaminants/html/1,3-Butadiene.htm, December 2004.
(11) Osterman-Golkar, S.; Bond, J. A. *Environ. Health Perspect.* **1996**, *104*, 907.
(12) Acquavella, J. F. *Toxicology* **1996**, *113*, 148.
(13) Kligerman, A. D.; Doerr, C. L.; Milholland, V. S.; Tennant, A. H. *Toxicology* **1996**, *113*, 336.
(14) Duffy, B. L.; Nelson, P. F. *Atmos. Environ.* **1996**, *30*, 2759.
(15) Shipp, A. M.; Allen, B. C. In *Toxic Air Pollution Handbook*; Patrick, D. R., Ed.; Van Nostrand Reinhold: New York, 1994; pp 79−99.
(16) Notario, A.; Le Bras, G.; Mellouki, A. *Chem. Phys. Lett.* **1997**, *281*, 421.
(17) Finlaysob-Pitts, B.; Pitts, J. N., Jr. *Chem. Upper Lower Atmos.* **2000**, 191.
(18) Seinfeld, J. H.; Pandis, S. N. *Atmos. Chem. Phys.* **1998**, 268.
(19) Wayne, R. P. *Chem. Atmos.* **2000**, 321.
(20) Atkinson, R. *Chem. Rev.* **1985**, *85*, 69. Atkinson, R. *Atmos. Environ.* **1990**, *24A*, 1.
(21) Atkinson, R.; Perry, R. A.; Pitts, J. N., Jr. *J. Chem. Phys*. **1977**, *67*, 3170.
(22) Liu, A.; Mulac, W. A.; Jonah, C. D. *J. Phys. Chem.* **1988**, *92*, 131.
(23) Tuazon, E. C.; Alvarado, A.; Aschmann, S. M.; Atkinson, R.; Arey, J. *Environ. Sci. Technol*. **1999**, *33*, 3586.
(24) Li, Z. *Chem. Phys. Lett.* **2004**, *383*, 592.
(25) Sander, S. P.; Friedl, R. R.; Golden, D. M.; Kurylo, M. J.; Huie, R. E.; Orkin, V. L.; Moortgat, G. K.; Ravishankara, A. R.; Kolb, C. E.; Molina, M. J.; Finlayson-Pitts, B. J. *Chemical Kinetics and Photochemical Data for Use in Stratospheric Modeling*; JPL Publication 02−25, **2003**.
(26) Frisch, M. J.; Trucks, G. W.; Schlegel, H. B.; Scuseria, G. E.; Robb, M. A.; Cheeseman, J. R.; Zakrzewski, V. G.; Montgomery, J. A., Jr.; Stratmann, R. E.; Burant, J. C.; Dapprich, S.; Millam, J. M.; Daniels, A. D.; Kudin, K. N.; Strain, M. C.; Farkas, O.; Tomasi, J.; Barone, V.; Cossi, M.; Cammi, R.; Mennucci, B.; Pomelli, C.; Adamo, C.; Clifford, S.; Ochterski, J.; Petersson, G. A.; Ayala, P. Y.; Cui, Q.; Morokuma, K.; Malick, D. K.; Rabuck, A. D.; Raghavachari, K.; Foresman, J. B.; Cioslowski, J.; Ortiz, J. V.; Baboul, A. G.; Stefanov, B. B.; Liu, G.; Liashenko, A.; Piskorz, P.; Komaromi, I.; Gomperts, R.; Martin, R. L.; Fox, D. J.; Keith, T.; Al-Laham, M. A.; Peng, C. Y.; Nanayakkara, A.; Challacombe, M.; Gill, P. M. W.; Johnson, B.; Chen, W.; Wong, M. W.; Andres, J. L.; Gonzalez, C.; Head-Gordon, M.; Replogle, E. S.; Pople, J. A. *Gaussian 98*; Gaussian, Inc.: Pittsburgh, PA, 1998. Head-Gordon, M.; Pople, J. A.; Frisch, M. J. *Chem. Phys. Lett*. **1988**, *153*, 503. Frisch, M. J.; Head-Gordon, M.; Pople, J. A. *Chem. Phys. Lett*. **1990**, *166*, 275. Frisch, M. J.; Head-Gordon, M.; Pople, J. A. *Chem. Phys. Lett*. **1990**, *166*, 281. Head-Gordon, M.; Head-Gordon, T.; *Chem. Phys. Lett*. **1994**, *220*, 122. Krishnan, R.; Pople, J. A. *Int. J. Quantum Chem.* **1978**, *14*, 91. R. Krishnan, R.; Binkley, J. S.; Seeger, R.; Pople, J. A. *J. Chem. Phys.* **1980**, *72*, 650. A. D. McLean, A. D.; Chandler, G. S. *J. Chem. Phys.* **1980**, *72*, 5639. Dunning, Jr., T. H. *J. Chem. Phys.* **1989**, *90*, 1007. Clark, T.; Chandrasekhar, J.; Spitznagel, G. W.; Schleyer, P. V. R. *J. Comput. Chem.* **1983**, *4*, 294.
(27) Atkinson, R.; Baulch, D. L.; Cox, R. A.; Crowley, J. N.; Hampson, R. F., Jr; Kerr, J. A.; Rossi, M. J.; Troe, J. *Summery of Evaluated Kinetic and Photochemical Data for Atmospheric Chemistry*. http://www.iupac-kinetic.ch.cam.ac.uk, March 2005. Holroyd, R. A.; Klein, G. W. *J. Phys. Chem.* **1963**, *67*, 2273. Adusei, G. Y.; Fontijn, A. *J. Phys. Chem.* **1993**, *97*, 1406. Weissman, M. A.; Benson, S. W. *J. Phys. Chem.* **1988**, *92*, 4080. Singleton, D. L.; Irwin, R. S.; Cvetanovic, R. J. *Can. J. Chem.* **1977**, *55*, 3321. Zellner, R.; Erler, K.; Field, D. *Symp. Int. Combust. Proc.* **1977**, *16*, 939. Arutyunov, V. S.; Buben, S. N.; Chaikin, A. M. *Kinet. Catal.* **1979**, *20*, 465. Zelenov, V. V.; Kukui, A. S.; Dodonov, A. F.; Aleinikov, N. N.; Kashtanov, S. A.; Turchin, A. V. Khim. Fiz. **1991**, *10*, 1221. Baulch, D. L.; Cobos, C. J.; Cox, R. A.; Esser, C.; Frank, P.; Just, Th.; Kerr, J. A.; Pilling, M. J.; Troe, J.; Walker, R. W.; Warnatz, J. *J. Phys. Chem. Ref. Data* **1992**, *21*, 411. Paulson, S. E.; Orlando, J. J.; Tyndall, G. S.; Calvert, J. G. *Int. J. Chem. Kinet*. **1995**, *27*, 997. Daby, E. E.; Niki, H.; Weinstock, B. *J. Phys. Chem.* **1971**, *75*, 1601.
(28) Atkinson, R.; Aschmann, S. M. *Int. J. Chem. Kinet* **1984**, *16*, 1175.
(29) Lloyd, A. C.; Darnall, K. R.; Winer, A. M.; Pitts, J. N., Jr. *J. Phys. Chem.* **1976**, *80*, 789.
(30) Chuong, B.; Stevens, P. S. *J. Phys. Chem. A* **2000**, *104*, 5230.
(31) Park, J.; Jongsma, C. G.; Zhang, R.; North, S. W. *J. Phys. Chem. A* **2004**, *108*, 10688.
(32) Peeters, J.; Boullsrt, W.; Pultau, V.; Vandenberk, S. *Proceedings of EUROTRAC Symposium 96* **1996**, *2*, 471. Greenwald, E. E.; Park, J.; Anderson, K. C.; Kim, H.; Reich, B. J. E.; Miller, S. A.; Zhang, R.; North, S. W. *J. Phys. Chem. A* **2005**, *109*, 7915.
(33) Almenningen, A.; Bastiansen, O.; Traetteberg, M. *Acta Chem. Scand.* **1958**, *12*, 1221.
(34) Steinfeld, J. I.; Francisco, J. S.; Hase, W. L. *Chemical Kinetics and Dynamics*; Prentice-Hall: 1999; p 287.
(35) Solomon, S.; Wuebbles, D.; Isaksen, I.; Kiehl, J.; Lal, M.; Simon, P.; Sze, N. *Scientific assessment of Ozone Depletion*; World Meteorological Organization report, Global Ozone Research and Monitoring Project-Report No. 37, 1995. Prinn, R.; Boldi, R.; Hartley, D.; Cunnold, D.; Alyea, F.; Simmonds, P.; Crawford, A.; Ramussen, R.; Fraser, P.; Gutzler, D.; Rosen, R. *J. Geophys. Res.* **1992**, *97* (D2), 2445.
(36) Atkinson, R. *J. Phys. Chem. Ref. Data* **1997**, *26*, 215.
(37) Díaz-Acosta, I.; Alvarez-Idaboy, J. R.; Vivier-Bunge, A. *Int. J. Chem. Kinet.* **1999**, *31*, 29.